BIOCHEMISTRY
including biophysical chemistry & molecular biology

Article

pubs.acs.org/biochemistry

Structure and Catalytic Regulatory Function of Ubiquitin Specific Protease 11 N-Terminal and Ubiquitin-like Domains

Stephen Harper,[†,#] Hayley E. Gratton,[†,#] Irina Cornaciu,[‡] Monika Oberer,[‡] David J. Scott,[§] Jonas Emsley,[†] and Ingrid Dreveny*[,†]

[†]Centre for Biomolecular Sciences, University of Nottingham, University Park Campus, Nottingham, NG7 2RD, United Kingdom
[‡]Institute of Molecular Biosciences, University of Graz, Humboldtstraße 50/3, A-8010 Graz, Austria
[§]School of Biosciences, University of Nottingham, Sutton Bonington Campus, Sutton Bonington, LE12 5RD, United Kingdom

Supporting Information

ABSTRACT: The ubiquitin specific protease 11 (USP11) is implicated in DNA repair, viral RNA replication, and TGFβ signaling. We report the first characterization of the USP11 domain architecture and its role in regulating the enzymatic activity. USP11 consists of an N-terminal "domain present in USPs" (DUSP) and "ubiquitin-like" (UBL) domain, together referred to as DU domains, and the catalytic domain harboring a second UBL domain. Crystal structures of the DU domains show a tandem arrangement with a shortened β-hairpin at the two-domain interface and altered surface characteristics compared to the homologues USP4 and USP15. A conserved VEVY motif is a signature feature at the two-domain interface that shapes a potential protein interaction site. Small angle X-ray scattering and gel filtration experiments are consistent with the USP11DU domains and full-length USP11 being monomeric. Unexpectedly, we reveal, through kinetic assays of a series of deletion mutants, that the catalytic activity of USP11 is not regulated through intramolecular autoinhibition or activation by the N-terminal DU or UBL domains. Moreover, ubiquitin chain cleavage assays with all eight linkages reveal a preference for Lys^{63}-, Lys^{6}-, Lys^{33}-, and Lys^{11}-linked chains over Lys^{27}-, Lys^{29}-, and Lys^{48}-linked and linear chains consistent with USP11's function in DNA repair pathways that is mediated by the protease domain. Our data support a model whereby USP11 domains outside the catalytic core domain serve as protein interaction or trafficking modules rather than a direct regulatory function of the proteolytic activity. This highlights the diversity of USPs in substrate recognition and regulation of ubiquitin deconjugation.

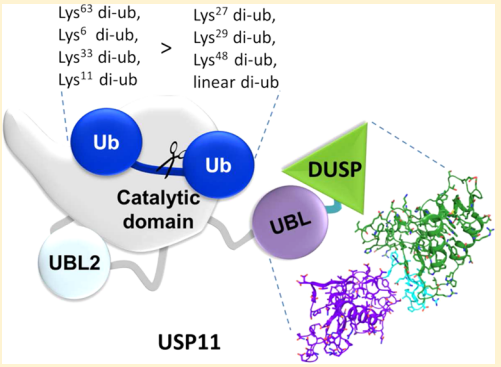

Ubiquitin specific proteases (USPs) contain a diverse range of ancillary domains,[1−4] whose roles are poorly characterized for the majority of USPs. They are likely to hold the key to specificity in terms of targeting these proteases to protein complexes and cellular compartments, serve regulatory functions, and play a role in substrate selectivity such as in the most well studied member of the USP family USP7/HAUSP.[5,6] The 105 kDa ubiquitin specific protease 11 (USP11) regulates vital signaling pathways in the nucleus. For example, USP11 acts as an upstream regulator of an IKKα-p53 signaling pathway[7] and interacts with the NF-κB transcription factor RelB. The scaffolding protein RanBPM and the breast cancer type 2 susceptibility protein (BRCA2) have been identified as a substrate for deubiquitination and an interaction partner respectively,[8,9] implicating USP11 in DNA damage repair. Indeed, USP11 exhibits pro-survival functions in the cellular response to DNA damage,[9] and RNA interference studies revealed that repair of DNA double-strand breaks by homologous recombination is defective in USP11-silenced cells.[10] A role of USP11 in transcriptional regulation by interacting with Polycomb complexes has also been identified,[11] and viral proteins such as human papillomavirus HPV-16E7 and influenza A viral RNA replication complex proteins interact with and can be substrates for USP11 deubiquitination.[12,13] Importantly, USP11 has been shown to exhibit altered expression levels in several types of cancers such as lung and breast cancer,[14,15] and the enzymatic activity of USP11 is inhibited by mitoxantrone which affects pancreatic cancer cell survival.[16] There is currently no structure for USP11 domains or information on how its catalytic activity is regulated and substrate is recognized.

USP11 is related by sequence to USP15 and USP4 referred to as the DUSP-UBL (DU) family of ubiquitin specific proteases that are predicted to share the same domain architecture harboring two internal ubiquitin-like (UBL) domains and an N-terminal domain present in ubiquitin-specific proteases (DUSP)[17] as shown in Figure 1A. The cysteine protease domains contain an insertion with a nested UBL domain (UBL2), which was proposed to possess an

Received: January 27, 2014
Revised: March 31, 2014
Published: April 11, 2014

   dx.doi.org/10.1021/bi500116x | *Biochemistry* 2014, 53, 2966−2978

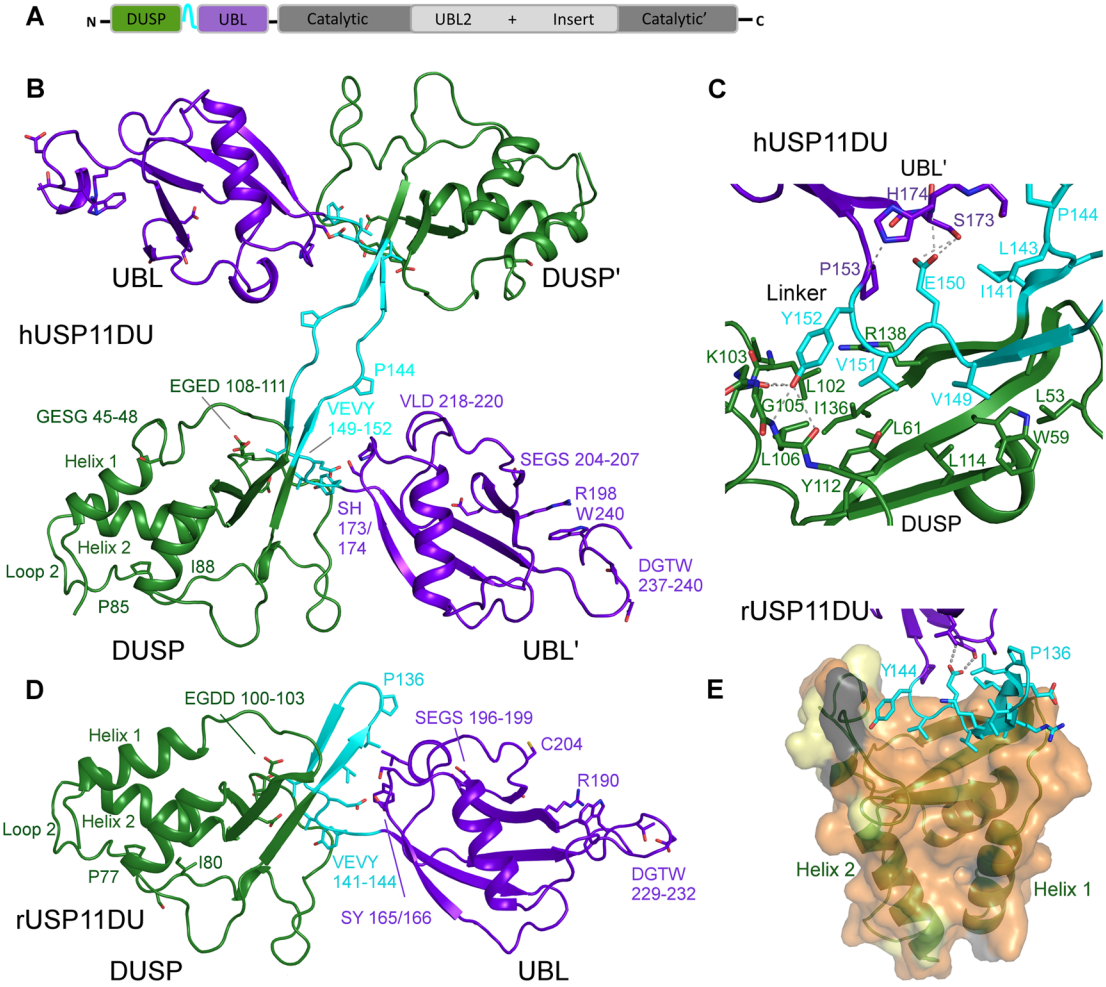

Figure 1. Structure of USP11 N-terminal DUSP-UBL domains. (A) Schematic representation of the USP11 domain structure. (B) Cartoon representation depicting human USP11DU in a dimeric domain swapped arrangement as observed in the crystallographic asymmetric unit. The second copy is labeled as ′. The DUSP domains from each chain are shown in green, the UBL domains are in purple, and the linker region, residues 141−152, is shown in cyan. (C) Close-up view of the DUSP−linker interaction in hUSP11. Note the VEVY motif, part of the linker region shown in cyan and the hydrophobic nature of side chains in the DUSP domain, shown in green. H-bonding interactions are indicated as dashed lines. (D) Cartoon depicting monomeric rat USP11DU in the same orientation as hUSP11DU in (B). The DUSP domain depicted in green stacks against the UBL domain from the same chain, shown in purple. This arrangement is mediated by the linker region, residues 133−144, which forms a β-hairpin structure denoted the DU finger. Key residues and sequence segments are labeled. (E) Cartoon depicting the hydrophobic DUSP-linker interface. The rUSP11 DUSP surface is colored according to sequence conservation between USP11 from human and rat. Identical residues are colored orange, residues that display similar properties are shown in yellow, and residues that are weakly similar in light gray and dissimilar in dark gray.

autoinhibitory function in USP4,[18] although the study supporting this has recently been retracted.[19] On the basis of these data and the role of UBL domains in USP7, it has been proposed that USP11 may also be regulated through its two internal UBL domains.[18] The N-terminal DUSP and UBL domains are more divergent than the catalytic core domains between USP4, USP11, and USP15 sequences and may additionally be involved in protein−protein interactions and targeting these proteases to different cellular compartments. In USP4 these domains mediate interactions with the spliceosomal recycling factor SART3[20] and the proteasomal subunit S9/Rpn6.[21] In USP15 an interaction with the E3 ligase BRAP was reported.[22] The crystal structures of the USP4 (Structural Genomics Consortium, unpublished) and USP15 N-terminal DU domains have been determined revealing a close association of the DUSP and UBL domains via a number of contacts and a β-hairpin DU finger structure.[23,24] In the more distantly related USP11, the predicted DUSP domain shares a moderate 39% sequence identity with the DUSP domains of USP15 and USP4 and the adjacent UBL domain only 32% sequence identity. A low resolution molecular envelope of these domains appears more extended compared to USP4 and USP15,[24] and it has been suggested that these domains adopt a different arrangement in USP11.[24] We were therefore interested in elucidating the atomic resolution structure of the USP11 DU domains. Although a number of USPs show only moderate ubiquitin chain specificity,[1] it is likely that both ubiquitin chain and target protein contribute to the overall specificity, and USPs may also aid in the recycling of these chains. It has been observed that USP11 can cleave isopeptide linked ubiquitin chains, but not linear diubiquitin.[1] How the USP11 DUSP and two internal UBL domains that may act as ubiquitin mimics contribute to catalysis and whether they possess a regulatory function are currently unknown. Tight regulation of USP activity is vital for the control of signaling pathways and protein degradation,[1,25] but research into USP

dx.doi.org/10.1021/bi500116x | *Biochemistry* 2014, 53, 2966−2978

Table 1. X-ray Data Collection and Refinement Statistics

data set	hUSP11DU		rUSP11DU	
space group	$P2_1$		$P22_12_1$	
a, b, c (Å)	27.7, 132.0, 72.0		37.3, 80.2, 149.3	
α, β, γ (deg)	90, 96.7, 90		90, 90, 90	
	all	outer shell	all	outer shell
resolution (Å)	48.51−2.90	3.06−2.90	54.62−2.34	2.42−2.34
R_{merge} [a]	0.116	0.83	0.152	0.963
R_{pim} [b]	0.040	0.290	0.049	0.300
CC1/2[c]	0.998	0.881	0.998	0.62
no. of total reflections	104271	15039	225549	22220
no. of unique reflections	11440	1689	19 709	1860
mean ((I)/sd(I))	13.9	3.3	13.1	2.9
completeness (%)	100	100	100	100
multiplicity	9.1	8.9	11.4	11.9
R_{work}/R_{free} [d]	0.231/0.297		0.221/0.264	
bonds (Å)	0.003		0.004	
angles (deg)	0.641		0.916	
Ramachandran outliers (%)	0		0	
Ramachandran favored (%)	95.5		97.7	
no. of residues	426		428	
average B factor protein (Å^2)	71.6		57.6	
no. of waters	4		53	
average B factor waters (Å^2)	56.8		56.9	
MolProbity score	1.73		1.41	

[a] $R_{merge} = \sum_h \sum_i |I_{i(h)} - \overline{I}_{(h)}| / \sum_h \sum_i I_{i(h)}$. [b] $R_{pim} = \sum_h (1/N-1)^{1/2} \sum_i |I_{i(h)} - \overline{I}_{(h)}| / \sum_h \sum_i I_{i(h)}$, h is the given reflection, $\overline{I}_{(h)}$ is the average intensity of each reflection and i is the ith measurement of reflection h. [c] CC1/2 is the Pearson correlation coefficient between random half-data sets. [d] $R_{work} = \sum_h |F_{obs(h)} - F_{calc(h)}| / \sum_h F_{obs(h)}$; R_{free} corresponds to the R_{work} based on 5% of the data excluded from refinement.

regulation mechanisms is at an early stage. In this study we undertook the first examination of the domain structure of USP11 and determined crystal structures of the human (hUSP11) and rat (rUSP11) USP11 N-terminal DU domains, analyzed potential interaction surfaces, USP11's oligomerization state and investigated the role of the ancillary domains in the catalytic activity and chain selectivity of USP11.

EXPERIMENTAL PROCEDURES

Cloning, Expression and Purification. Full-length human USP11, residues 1−920 (FL-USP11), and a range of deletion mutants including 24−244 (hUSP11DU), 1−445/736−920 (FLΔUBL2), and 252−445/736−893 (CatΔUBL2) were amplified from I.M.A.G.E. clone 4180680. In the ΔUBL2 constructs a 290-residue deletion is substituted by a short linker, based on USP8 (PDB code 2GFO) residues 957−961 ASTSK, which connects residues 445 and 736. The N-terminal region from the rat USP11 gene encoding residues 19−236 (rUSP11DU) was amplified from I.M.A.G.E. clone 7190710. CatΔUBL2, hUSP11DU, and rUSP11DU were cloned into pET26b using NdeI and XhoI restriction sites. FL-USP11 and FLΔUBL2 were cloned into pCold1 using NdeI and *Hin*dIII restriction sites. The human ubiquitin sequence was inserted into pRSF-13 (Arie Geerlof, EMBL Hamburg, Germany) using NcoI and *Hin*dIII restriction sites. Protein expression was induced by adding 0.5 mM IPTG to BL21-CodonPlus cells grown at 37 °C in 2xYT medium to mid log phase. Cells harboring the hUSP11DU plasmid were harvested after 4 h. For rUSP11DU and CatΔUBL2 expression, cells were grown at 20 °C for 16 h before harvesting, and for FL-USP11 coexpressed with ubiquitin and FLΔUBL2 expression, cells were grown for 72 h at 10 °C prior to centrifugation. For rUSP11DU, hUSP11DU, and the CatΔUBL2 construct, cells were lysed by sonication in 20 or 50 mM Tris-Cl pH 7.5, 150 mM NaCl, 20 mM imidazole. Cells containing FL-USP11 and FLΔUBL2 were lysed in 50 mM Tris-Cl, 300 mM NaCl, 5% (v/v) glycerol, 20 mM imidazole. Samples were purified using HiTrap chelating columns (GE Healthcare) precharged with nickel sulfate. rUSP11DU, hUSP11DU, and CatΔUBL2 were further purified by size exclusion chromatography on a Superdex 75 16/60 column (GE Healthcare) pre-equilibrated with 50 mM Tris-Cl, pH 7.5, and 150 mM NaCl. FL-USP11 and FLΔUBL2 were further purified using a Superdex 200 16/60 column (GE Healthcare), pre-equilibrated with 50 mM Tris-Cl, pH 7.5, 300 mM NaCl, and 1% glycerol.

Crystallization. Crystallization trials of hUSP11DU and rUSP11DU were carried out using the hanging drop vapor diffusion method. The best diffracting crystals for hUSP11DU grew in Morpheus screen[26] condition C4 containing 0.1 M MES/imidazole pH 6.5, 30 mM sodium nitrate, 30 mM sodium phosphate, and 30 mM sodium sulfate, 12.5% (w/v) PEG1000, 12.5% (w/v) PEG3350, 12.5% (v/v) MPD at a protein concentration of 10 mg mL^{-1}. The crystals grew in less than 1 week and had a plate-like morphology. The best diffracting rUSP11DU crystals grew within 2 days at 7.5 mg mL^{-1} in a condition based on JCSG+ condition G8 containing 0.15 M malic acid pH 6.8, 24% (w/v) PEG3350, and 10 mM strontium chloride hexahydrate.

Data Collection, Structure Determination, and Refinement. Data from hUSP11DU crystals were collected on the microfocus beamline ID23-2 at the ESRF, France. Data were processed using iMosflm, and four data sets from the same crystal were scaled together using Aimless (CCP4 suite[27]). The structure was solved by molecular replacement in Phaser using the USP4 DUSP and UBL domains (PDB code 3JYU; SGC) as search models.[28] The final model was generated through

dx.doi.org/10.1021/bi500116x | *Biochemistry* 2014, 53, 2966−2978

iterative rounds of model building in COOT and refinement using Phenix,[29] with noncrystallographic symmetry restraints (NCS) and translation/libration/screw (TLS) groups from the TLSMD server used in the final rounds of refinement.[30] The first nine residues and the His-tag of the hUSP11DU construct were not observed in the density and omitted from the final model. Nine surface residue side chains could not confidently be modeled and were truncated at the Cβ position; these comprise residues Gln^{95}, Arg^{101}, Asn^{203}, Lys^{235}, Lys^{236} from chain A and residues Glu^{187}, Arg^{188}, Asn^{203}, Lys^{236} from chain B.

Data from a rUSP11DU crystal were collected at beamline ID29 at the ESRF, France. Data were processed using XDS[31] and scaled using Aimless.[27] The structure was solved by molecular replacement with Phaser using the DUSP and UBL domains from the hUSP11DU structure individually as search models. Restrained refinement using TLS groups was carried out in Refmac and Phenix[27,29] using NCS restraints. The first seven and eight residues in chain A and B, respectively, were not clearly defined in the electron density and therefore not modeled. The side chain of Glu^{197} was truncated due to flexibility. The two copies in the asymmetric unit are linked by a nonphysiological disulfide bond formed between Cys^{204} in both copies. Data collection and refinement statistics are listed in Table 1. Atomic coordinates and structure factor files were deposited at a member site of the Protein Data Bank (www.rcsb.org) under accession codes 4MEL (hUSP11DU) and 4MEM (rUSP11DU).

Small Angle X-ray Scattering and Differential Scanning Calorimetry. Data of hUSP11DU samples were collected at 7.6, 3.8, and 1.9 mg mL^{-1} in 50 mM Tris-Cl, pH 7.4, 150 mM NaCl at beamline X33 at the DORIS-III storage ring at DESY, Germany. Buffer subtracted curves were processed using the program Primus.[32] The radius of gyration, R_g, was determined using the Guinier approximation at very low scattering angles using 64 data points (72−135) from the merged buffer subtracted curves which fell within the accepted range of $0.6 < qR_g < 1.3$. The D_{max} was determined from the distance distribution $p(r)$ function using the program Gnom.[33] *Ab initio* model building was carried out using the program DAMMIN. The DAMAVER program was used to produce an average model and create a solvent reduced molecular envelope from 15 independent *ab initio* models built in DAMMIN followed by DAMFILT for filtering to obtain a representative dummy atom model.[32] The hUSP11DU crystal structure with the domain swapped dimer and a monomeric model was used to generate theoretical scattering curves in CRYSOL. The hUSP11DU monomeric model was created to generate a single chain with a DU finger β-hairpin by superimposing the individual DUSP and UBL domains onto the rUSP11DU structure and replacing the coordinates of hUSP11DU residues 143−148 with the coordinates of residues 135−140 from rat with the human sequence. These models were fitted into the *ab initio* molecular envelope using the program Chimera.[34]

For differential scanning calorimetry (DSC), 2 mg mL^{-1} h USP11DU, hUSP15DU, and hUSP4DU were dialyzed into PBS buffer, 10 mM phosphate buffer, 2.7 mM KCl, 137 mM NaCl pH 7. Data were collected on a Microcal VP-DSC calorimeter at a scan rate of 1 °C min^{-1} with a low feedback mode/gain. Data were analyzed using the Origin 7.0 software (MicroCal). All DU domain samples unfolded irreversibly and visibly aggregated following thermal denaturation.

Kinetic Assays and Diubiquitin Chain Selectivity Assay. Deubiquitination assays were performed with human FL-USP11, FLΔUBL2, and CatΔUBL2 at a concentration of 75 nM enzyme and 0.1 μM to 1.5 μM ubiquitin-AMC (7-amino-4-methylcoumarin) as the fluorogenic substrate. Reactions were carried out in 150 mM NaCl, 50 mM Tris-Cl pH 7.5, 1 mM DTT, in 384-well black plates (Nunc) with 30 μL final volumes in triplicate. Plates were read with an EnVision 2104 multilabel plate reader at 25 °C using excitation wavelength 355 nm and emission wavelength 426/428 nm. Measurements were taken every minute for the first 20 min, then every 2 min for the next 30 min, and subsequently at increasing intervals of 5, 10, and 20 min. Curves containing 15 data points measured in triplicate were fitted using nonlinear regression analysis in GraphPad prism software to establish K_m and k_{cat} values.

Diubiquitin chain cleavage assays were performed with all three proteins at a concentration of 75 nM enzyme with 5 μM of the eight diubiquitin linkage types: linear, Lys^{6}, Lys^{11}, Lys^{27}, Lys^{29}, Lys^{33}, Lys^{48}, and Lys^{63} (Viva Bioscience). Reactions were carried out in 150 mM NaCl, 50 mM Tris-Cl pH 7.5, 1 mM DTT at 23 °C in duplicate. Five microliter samples were taken at 0, 5, 10, 30, 60, 120, and 180 min with a final sample taken at 19 h. Reactions were stopped by the addition of SDS-PAGE loading buffer and analyzed on Novex Tris-Glycine 18% SDS-PAGE. Gels were stained with Coomassie blue followed by EZBlue. Gels were scanned and then analyzed with the ImageJ software where relative amounts of diubiquitin and mono-ubiquitin for each time point were determined. The mean diubiquitin percentage was calculated from duplicate SDS-PAGE gels and plotted using GraphPad Prism software using nonlinear regression analysis.

RESULTS

Structures of Human and Rat USP11 N-Terminal DU Domains. To investigate the structure of USP11, we initially focused our attention on the N-terminal DU domains as we observed these domains as a common breakdown product during expression and in limited proteolysis experiments with full-length USP11. We therefore cloned human USP11 N-terminal constructs spanning residues 1−244 and 24−244 harboring the predicted DUSP and UBL domains. The first 23 residues are highly alanine rich and are predicted to be disordered using the RONN server,[35] and we only obtained crystals with the latter construct. In order to potentially obtain a higher resolution structure and investigate the evolutionary conservation of USP11, we also designed an analogous N-terminal construct for the rat ortholog (residues 19−236) for which we also obtained diffraction quality crystals. The structures were solved using molecular replacement and statistics are summarized in Table 1.

The 2.9 Å structure of hUSP11DU shows that the two copies in the asymmetric unit pack in a domain swapped dimeric arrangement (Figure 1B) via an extended linker region (residues 141−152) in the crystal. The first ∼110 N-terminal residues adopt a three helix bundle stacked against a three-strand antiparallel β-sheet adopting the DUSP fold first characterized in USP15.[36] A distinctive feature in the DUSP domain of hUSP11 compared to other DUSP structures is that in the N-terminal helix 1 residues 45−48, GESG, break the helix after two turns creating a short loop where Glu^{46} and Ser^{47} are solvent exposed and not engaged in crystal contacts. Loop 2 (L2) comprising residues Gly^{76}-Asp^{111} in hUSP11 (Figure 1B) is tethered to the DUSP surface by interactions from residues Pro^{85} and Ile^{88} with Trp^{66} from α-helix 2. These residues form

dx.doi.org/10.1021/bi500116x | *Biochemistry* 2014, 53, 2966−2978

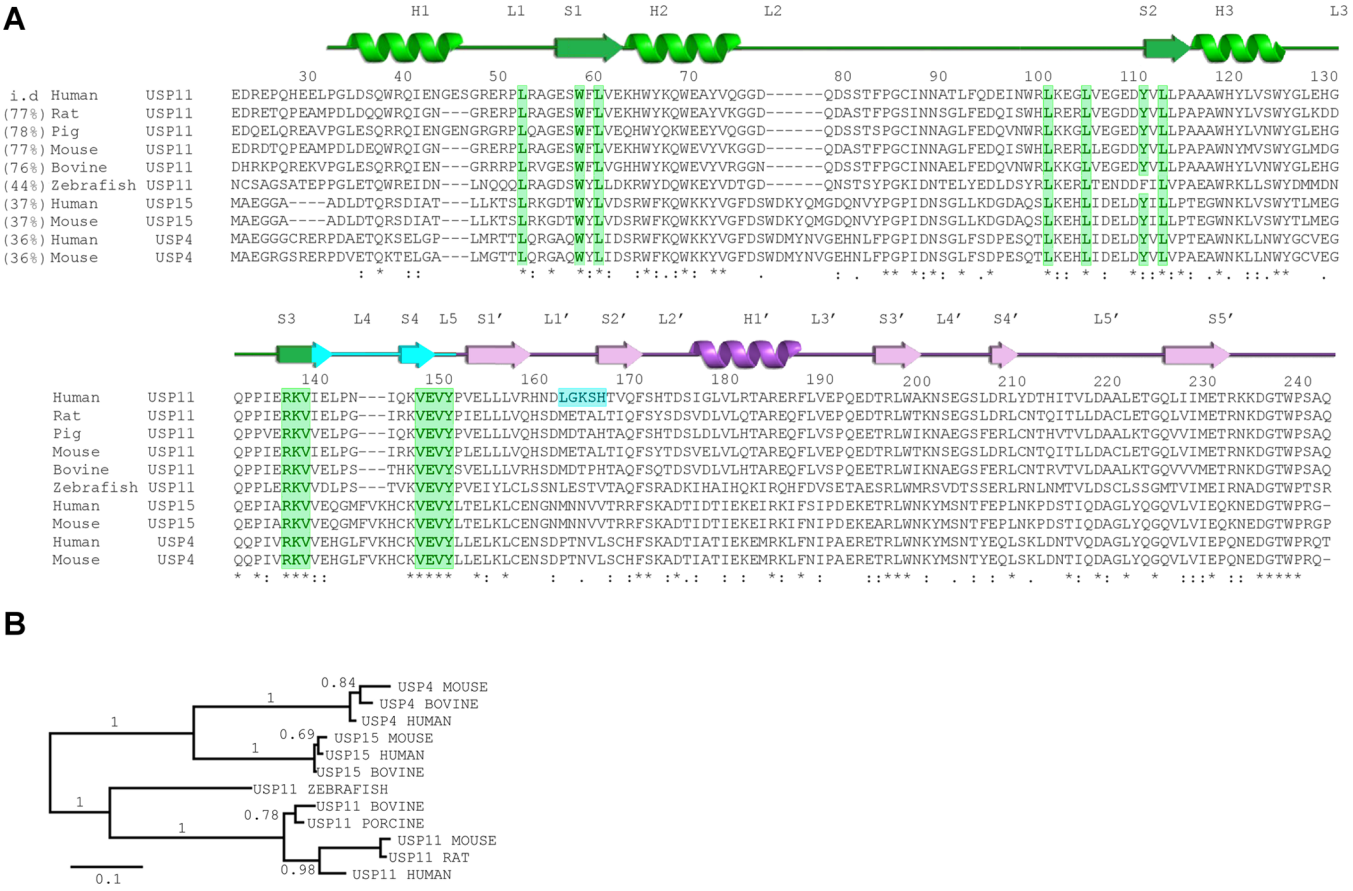

Figure 2. Sequence conservation in USP11 and the homologues USP15 and USP4. (A) Multiple sequence alignment of the N-terminal DUSP-UBL domain region of human USP11 (UniProt P51784), porcine USP11 (UniProt F1RWV6), mouse USP11 (UniProt Q99K46), bovine USP11 (UniProt A5PKF9), rat USP11 (UniProt Q5D006), zebrafish USP11 (UniProt F1QPF4), human USP15 (UniProt Q9Y4E8), mouse USP15 (UniProt Q8R5H1), human USP4 (UniProt Q13107) and mouse USP4 (UniProt P35123) generated using Clustal Omega. Residue numbers and secondary structure elements are based on the structure of hUSP11DU assigned using the PDBsum server at the EBI. Sequence identity of respective sequences shared with human USP11 are given in brackets. α-Helices (H) and β-strands (S) from the UBL domain are renumbered to match nomenclature for ubiquitin and as such are denoted S′ or H′. Residues involved in the DUSP-linker interface described in Figure 1C are highlighted in green. The loop connecting strand S1′ and S2′ of the UBL domain (shown in blue) is not conserved in other USP11 sequences. (B) Phylogenetic analysis of members of the DU family show that the evolutionary divergence is greater among USP11 orthologues compared to USP15 and USP4 orthologues.

part of the signature PGPI sequence identified by bioinformatic analysis as being shared by DUSP domains from seven distinct USPs,[36] but the second proline is substituted by Cys[87] in hUSP11DU. Prior to strand S2 there is a turn spanning residues Glu[108]-Asp[111] that contains several acidic residues with the sequence EGED. This loop forms the central feature of a cleft, which involves residues on the surface of the DUSP domain and includes part of the interface between the DUSP and the interdomain linker region (Figures 1 and 3F). In the crystal, the linkers between the DUSP and UBL domains form an antiparallel β-sheet which is interrupted at the center by Pro[144] in such a way that the DUSP domain from one chain stacks against the UBL domain from the other (Figure 1B,C). Representative electron density for the linker region is shown in Figure S1A (Supporting Information). The DUSP domain is anchored to the linker region by an extensive predominantly hydrophobic interface which involves 14 residues covering 1508 Å^2 in hUSP11DU (PISA server at the EBI[37]). The interaction is dominated by a conserved VEVY motif in the linker where the two valine residues, Val[149] and Val[151], are almost completely buried (Figure 1C).

Residues 154−244 adopt a β-grasp ubiquitin-like fold with a second short helical turn inserted between strands 4′ and 5′ comprising residues 218−220 (Figure 1B). The UBL domain is anchored to the linker region by Glu[150] from this VEVY motif (Figure 1C) through side chain mediated hydrogen bonds with Ser[173] and the backbone amine of the upstream residue His[174]. Residue Tyr[152] from the VEVY motif positioned prior to the bridging residue to the UBL domain, Pro[153], forms hydrogen bonding interactions with main chain groups from Lys[103] and Leu[106]. The side chain of His[174] forms a hydrogen bond with the main chain carbonyl of Tyr[152] (Figure 1C). Interchain interactions between Ile[141], Leu[143], and Thr[175], Leu[219] are also seen. These interactions are the only contacts between the UBL domain to either the linker or the DUSP domain.

Clearly identifiable USP11 orthologues are only found in vertebrates, and USP11 is less conserved across species compared to USP4 and USP15 (Figure 2A,B). hUSP11DU and rUSP11DU share 76.1% sequence identity, and the two DUSP domains can be aligned with an RMSD of 0.7 Å and the UBL domains with an RMSD of 1.5 Å. Interestingly, in the 2.3 Å crystal structure of USP11 from rat (rUSP11DU) the linker region (residues 133−144) forms a β-hairpin capped by a type

dx.doi.org/10.1021/bi500116x | Biochemistry 2014, 53, 2966−2978

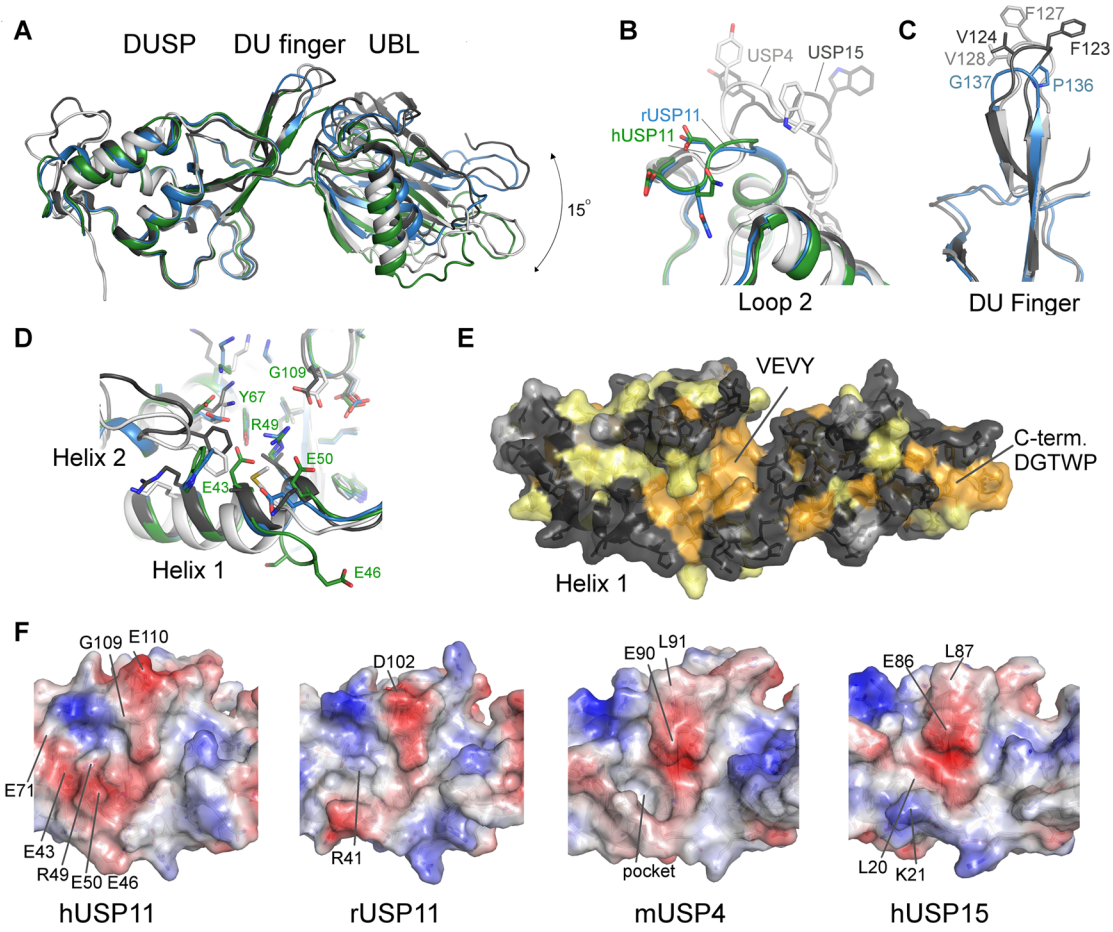

Figure 3. Structural features of USP11, USP4, and USP15 DU domains. (A) Superposition of the structures of hUSP11DU (green), rUSP11DU (blue), hUSP15DU (dark gray, PDB code 3T9L[23]), mUSP4 (light gray, PDB code 3JYU, SGC). The structures are aligned using the DUSP domain as reference and show that the relative orientation of the UBL domain varies by approximately 15 degrees. Several important surface features are highlighted in close-up views in B, C, and D. (B) Loop 2 following helix 2 in the DUSP domain is locally the most structurally diverse region in members of the DU family. (C) The DU finger region in rUSP11 is three residues shorter than in USP15 and USP4 and is capped by a proline and glycine residue, whereas in USP15 and USP4 the fingertip harbors phenylalanine and valine residues. (D) Helix 1 in the DUSP domain is three residues longer in hUSP11 compared to rUSP11 and other members of the DU family. A GESG motif breaks the helix. Residues in helix 1 may be functionally significant as they contribute to a hydrophobic cleft on the DUSP surface in hUSP15 and mUSP4. The presence of an arginine (R49) and two glutamic acid residues (E43, E50) significantly alter the physicochemical properties of this surface feature in hUSP11DU. (E) Surface representation of the rUSP11DU structure colored according to sequence conservation in USP11, USP4, and USP15. Identical residues are colored orange, similar residues yellow, weakly similar in light gray, and dissimilar in dark gray. (F) Surface representations colored according to electrostatic potential of the DUSP domain cleft region in hUSP11, rUSP11, hUSP15, and mUSP4 with the same face of the DUSP domain shown as in (D) and (E). Residues not conserved between the structures that contribute to different surface characteristics are labeled as well as the deep hydrophobic pocket in USP4.

II β-turn with residues Pro^{136} and Gly^{137} at its center (highlighted in cyan in Figures 1D,E and Figure S1B, Supporting Information). This turn causes the DUSP and UBL domains to pack in a side by side tandem arrangement mediated by a small interface comprising ~200 Å^2 (Figure 1D,E). Nevertheless, in rUSP11DU, the DUSP and linker region form an equivalent interface to that of hUSP11DU (Figure 1C,E). In the rUSP11DU structure, this involves residues from the same chain due to the formation of the β-hairpin DU finger (termed in analogy to the homologue USP15[23]) as opposed to involving a second chain in the domain swapped arrangement of the hUSP11DU crystal structure. The majority of structural features are conserved such as the acidic loop in the DUSP domain (residues 100−103 EGDD) and hydrophobic contacts at the two domain interface involving Ile^{133} and Leu^{135} from the DU finger region and Ser^{167} and Leu^{211} in the UBL domain in rUSP11. hUSP11DU His^{174} is replaced by Tyr^{166} in the rUSP11DU structure at the interface, but the VEVY motif is conserved. However, despite the significant sequence similarities, some DU surface features are not conserved. In the rUSP11DU structure, Pro^{136} and Gly^{137} form the DU finger β-turn, whereas the equivalent hUSP11DU residues Pro^{144} and Asn^{145} are at the center of the linker in the crystal structure. The hUSP11 DUSP domain contains a three residue insertion in the N-terminal α-helix, not present in known USP11 sequences from most other species including rat (Figure 2A). In rUSP11DU, α-helix 1 has three turns, lacking this insertion. It is possible that these residues mediate protein−protein interactions specific to hUSP11. Glu^{43} in hUSP11DU preceding this insertion in α-helix 1 is substituted by a glycine, Gly^{38}, in rat. The acidic residue contributes to this otherwise conserved DUSP surface cleft formed by α-helix 1, α-helix 3, and β-strand, S2 (Figures 3D,F and S2B). The surface exposed loop which connects strand S1′ and S2′ in the UBL

dx.doi.org/10.1021/bi500116x | *Biochemistry* 2014, 53, 2966−2978

domain is also variable in sequence and surface charge (Figure 2A) between rat and human USP11. The position of the UBL domain relative to the DUSP domain varies by up to 15 degrees between molecules, mainly mediated through a hinge point at the start of the UBL domain following a proline (Pro[145] in rat or Pro[153] in human), Figure 3A.

Ubiquitin (DALI Z score 11.3, PDB code 1TBE, 15% seq id.) and the related modifier ISG15 (Dali Z-score 11.7, PDB code 3PHX, 18% seq id., 1.4 Å RMSD) are identified as the closest structural neighbors to the USP11 UBL domain excluding the homologous USP4 and USP15 UBL structures using a database search with DALI.[38] Despite poor sequence conservation, 15.8% and 11.8% sequence identity with the human and rat USP11 UBL domain respectively, the domains align to ubiquitin (PDB code 1UBQ[39]) with an RMSD of 1.6 Å over 70 Cα positions. The main structural difference between the USP11 UBL domain and ubiquitin involves the presence of a longer loop region between strands S3′ and S4′ comprising the sequence SEGS (Figure 1B,D). This loop region is often involved in protein−protein interactions in UBL domains.[40]

None of the lysine residues or surface features described in ubiquitin are well conserved in the USP11 UBL domain of the DU module. Asp[220] in hUSP11 occupies a structurally equivalent position as Asp[58] in ubiquitin, but other residues in the polar patch are not conserved. At the position of residues equivalent to the hydrophobic patch in ubiquitin, Ile[44] is substituted by a bulky tryptophan residue, Trp[200], while other residues in this hydrophobic patch region are buried by the hUSP11 C-terminus of the UBL domain. In contrast to the ubiquitin C-terminal diglycine motif, the hUSP11 UBL C-terminus adopts a turn involving the sequence DGTWP where Trp[240] forms a π-stacking interaction against the side chain of Arg[198] (Figure 1B).

Comparison of USP11 with the Homologues USP4 and USP15. USP4 and USP15 are overall less than 40% identical in sequence to USP11, but there is some functional overlap in the involvement of these enzymes in TGFβ signaling.[41−44] Common binding partners between USP11, USP15, and USP4 are not known at present.[45] The two USP11 DU structures allow us to define hallmarks of the DUSP-UBL module in USP4, USP15, and USP11 as well as delineating the characteristics of USP11. The structure of the hUSP11 DUSP domain can be superimposed onto the structure of hUSP15DU, PDB code 3T9L[23] with an RMSD of 1.2 Å over 103 Cα positions (seq id. 44%) and the UBL domains with an RMSD of 1.1 Å over 98 Cα positions (seq id. 34%). Similarly, the hUSP11 DUSP domain aligns to the structure of murine USP4DU, PDB code 3JYU (SGC) with an RMSD of 1.3 Å over 103 Cα positions (seq id. 41%) and an RMSD of 1.6 Å over 99 Cα positions for the UBL domain (seq id. 33%), respectively.

We reported a β-hairpin structure at the interface of the two domains denoted the DU finger in USP15,[23] which is also observed in the USP4DU structure (PDB code 3JYU, SGC). Unexpectedly, in the rUSP11DU structure a tight turn is observed aided by Pro[136] and Gly[137] to preserve the β-hairpin despite a three residue deletion in the DU finger region compared to USP15 and USP4. In USP15 and USP4 the turn involves five residues and is topped by phenylalanine residues that are conserved among USP15 and USP4 orthologues[23,24] (Figure 3C). A domain swapped dimeric arrangement has been observed in one of the available hUSP15DU structures (PDB code 3PV1[24]), highlighting that under certain conditions DU finger opening can occur, and a strand from another molecule can complete the antiparallel β-sheet of the β-hairpin. It is curious that in our USP11 as well as a USP15 DU structure, this opening is observed through "peeling off" of the VEVY motif to be replaced by the same motif of another molecule independent of the different lengths of the DU finger. Whether this purely represents a crystallographic artifact or has any functional significance remains to be determined.

Eight out of nine hydrophobic residues defining the DUSP domain-linker interactions including the VEVY motif are absolutely conserved in all of the USP15, USP4, and USP11 sequences (Figure 2A). The only other absolutely conserved region in the USP11, USP15, and USP4 N-terminal domains not contributing to the hydrophobic core constitutes the C-terminal DGTWP motif that loops back onto the UBL domain (Figures 1B,D and 3E). Loop 2 is one of the most variable regions among the DU family of USPs (Figures 2A, 3B, and S2A; Supporting Information) and is six residues shorter in USP11 compared to USP15 and USP4. USP11 thus lacks solvent exposed tryptophan and tyrosine residues present in USP4 and USP15.

A relatively hydrophobic crescent shaped cleft (Figure 3F) may constitute a potential protein−protein interaction site in the USP4 and USP15 DUSP domain structures.[23,24] In USP4, Phe[127] at the tip of the DU finger extends into a deeper hydrophobic pocket at this location in a second copy of the protein in the asymmetric unit (Figure 3F). In hUSP11 this region is also predominantly hydrophobic, but several surface exposed residues from helix 1, helix 2 and surrounding residues are not identical in this region (Figures 3D,F and S2B; Supporting Information). These include Tyr[67], which is substituted by Phe[38] and Phe[42] in USP15 and USP4, respectively, and forms a hydrogen bond with Glu[43] and Arg[49] in hUSP11 (Leu[20] and Met[24] in USP15 and USP4 respectively) and Glu[46]. In USP11, the side chain of Arg[49] fills the respective deep hydrophobic pocket where in USP4 the side chain of Phe[127] is buried (Figures 3D and S2B; Supporting Information). In this area, there are also differences in charge whereby Glu[71] (USP15 Lys[42], USP4 Lys[46]) forms an additional hydrogen bond to the conserved surface exposed Lys[68] in USP11. At the position of Gly[109], USP15 and USP4 harbor glutamic acid residues.

In order to better understand the solution behavior of the DU domains, we conducted thermal unfolding studies using differential scanning calorimetry (Figure S3F, Supporting Information). USP11, USP15, and USP4 DU domains each display a melting transition with a single peak, suggesting that the dissociation between the DUSP and UBL domains either produces insufficient heat to be measured by the method or occurs simultaneously with thermal unfolding of both domains. Notably, the melting transition was significantly different between USP15 and the closely related USP4 constituting a 7 °C shift in temperature and thus was not dependent on the DUSP-UBL interface area.

The USP11 DUSP-UBL Domains and Full-Length USP11 Are Monomeric in Solution. The occurrence of the domain swapped dimeric arrangement in the human USP11DU crystal structure raised the question about the predominant form in solution. During purification USP11DU elutes on size exclusion column at a volume consistent with a monomer in agreement with SEC-MALLS experiments.[24] At concentrations associated with crystallization we see a small, about 5%, fraction of dimeric hUSP11DU on gel filtration. In order to further investigate the oligomeric state of hUSP11DU

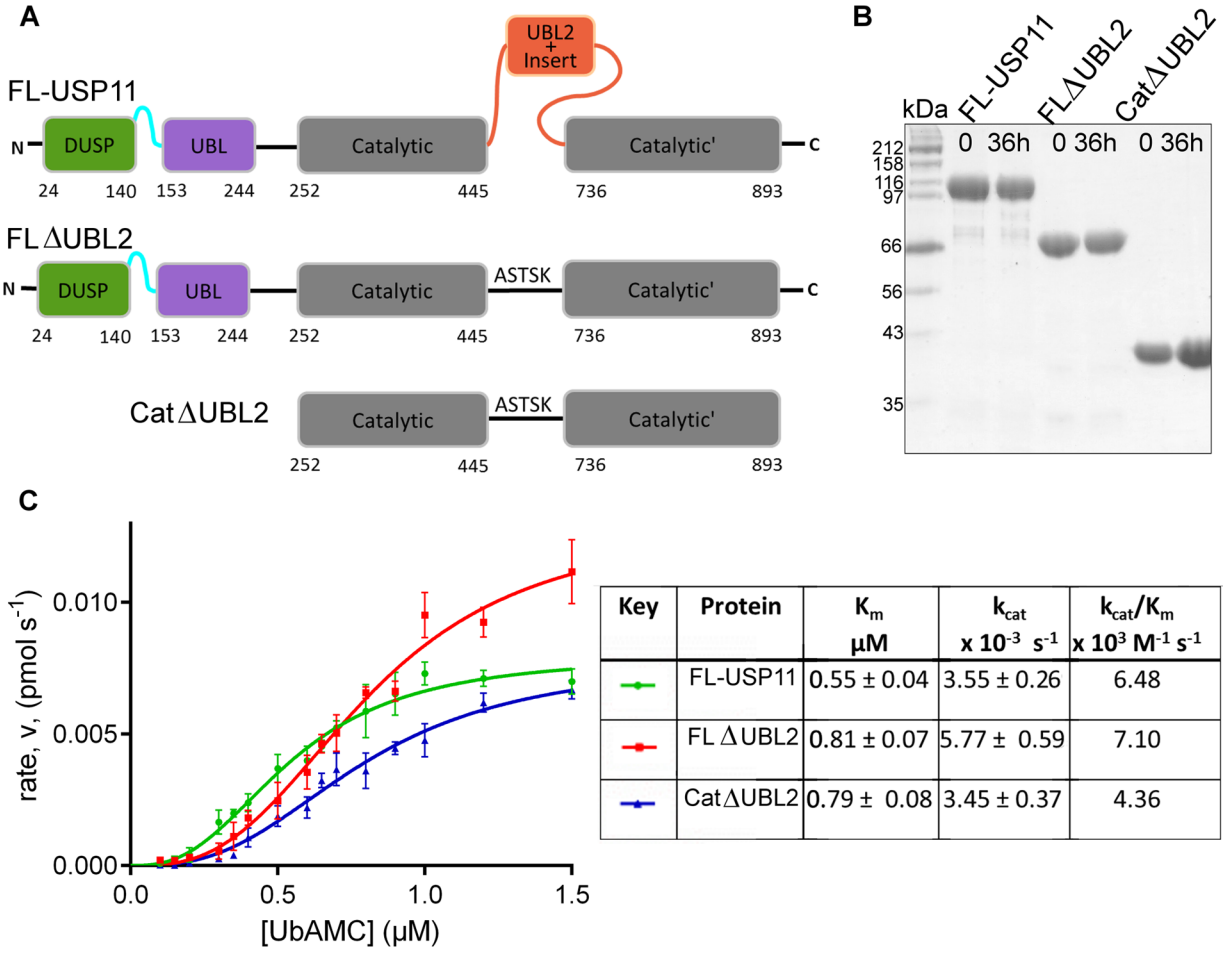

Key	Protein	K_m μM	k_{cat} x 10^{-3} s^{-1}	k_{cat}/K_m x 10^3 M^{-1} s^{-1}
	FL-USP11	0.55 ± 0.04	3.55 ± 0.26	6.48
	FL ΔUBL2	0.81 ± 0.07	5.77 ± 0.59	7.10
	Cat ΔUBL2	0.79 ± 0.08	3.45 ± 0.37	4.36

Figure 4. Kinetic parameters for USP11 and deletion mutants. (A) Schematic representation of the hUSP11 constructs used in the activity assays. FL-USP11: full-length enzyme; FLΔUBL2: missing the UBL2 and insert nested in the catalytic domain; CatΔUBL2: additionally lacking the N-terminal DUSP and UBL domains. Deletion mutants lacking the UBL2 and insert have been replaced with a linker from USP8. (B) SDS-PAGE analysis of samples of FL-USP11 (107 kDa, lanes 2 and 3), FLΔUBL2 (77 kDa; lanes 4 and 5) and CatΔUBL2 (42 kDa; lanes 6 and 7), before the assays (time 0) and after the assay (time 36 h). (C) Graph of rate of reaction against substrate concentration for FL-USP11 (green), FLΔUBL2 (red) and CatΔUBL2 (blue). Each point represents the mean for data points measured in triplicate. Values for V_{max} and K_m were used to calculate the turnover number, k_{cat}, and catalytic efficiency k_{cat}/K_m and are listed in the table. Errors are given as standard error mean.

in solution, we used small-angle X-ray solution scattering. USP11DU has a radius of gyration (R_g), calculated from the Guinier plot, of 27.8 Å. From a $p(r)$ function a maximum dimension (D_{max}) of 97.2 Å was estimated. *Ab initio* model building resulted in molecular envelopes consistent with a two domain structure of a hUSP11DU monomer, with insufficient space to accommodate a dimer. Using the hUSP11 structure, where a DU finger β-hairpin based on the rUSP11DU structure was modeled, resulted in a good fit, and the theoretical and experimental scattering curves agree (Figure S3A–E, Supporting Information). The additional volume in the molecular envelope can be explained by the hydration shell and flexible residues at the N- and C-termini that are not present in the crystal structure.

For hUSP15DU, an R_g of 26.6 Å and a D_{max} of 81 Å have been reported.[23] The presence of a DU finger β-hairpin in the rUSP11DU structure and the conservation of the DUSP-linker interface in the hUSP11DU structure suggest that the differences are most likely due to the relative orientation of the UBL domain, an additional four residues at the N-terminus compared to USP15, and a flexible C-terminal His-tag that all contribute to the apparent D_{max} and R_g. Furthermore, we investigated the oligomerization state of full-length hUSP11 using gel filtration which showed that full-length hUSP11 is monomeric in solution (Figure S3G, Supporting Information).

Influence of the USP11 DUSP-UBL and UBL2 Domains on the Catalytic Function. As UBL domains have been shown to modulate USP activity,[5,18,46,47] we were interested in whether the DUSP-UBL module or the UBL2 domain of USP11 have an effect on the catalytic activity. In order to investigate the role of USP11 ancillary domains in regulating the catalytic activity, we designed and cloned several deletion constructs of USP11 that contain the protease domain (Figure 4A). The overall yield for full-length USP11 (FL-USP11) was poor, but pure and stable protein suitable for assays was obtained (Figure 4B). Deletion constructs lacking either the DUSP domain alone or the N-terminal DUSP-UBL domains had a very low level of expression and were prone to precipitation and as such were not further utilized. However, we obtained pure protein of around 2 mg L^{-1} of culture by replacing the UBL2 containing insert with a short linker. A further construct suitable for assays was obtained by removal of the DUSP-UBL domain from the ΔUBL2 fusion construct (Figure 4A,B).

dx.doi.org/10.1021/bi500116x | *Biochemistry* 2014, 53, 2966–2978

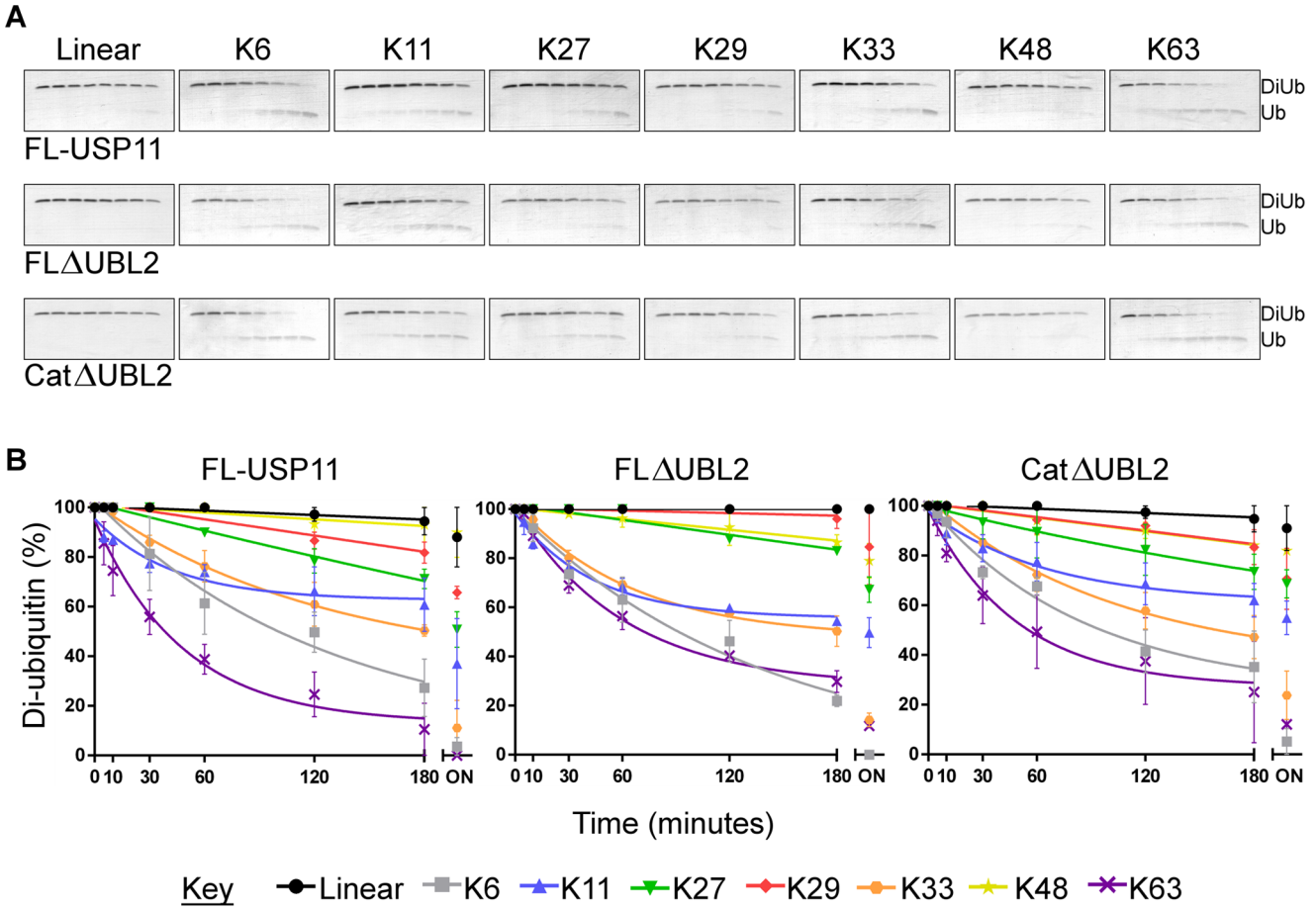

Figure 5. Ubiquitin chain selectivity. (A) SDS-PAGE analyses of cleavage of diubiquitin to monoubiquitin by USP11 and deletion mutants with the eight linkage types (as labeled). Assays were performed in duplicate and representative gels are shown. The lanes on each gel show a time course of a reaction with 75 nM USP11 and 5 μM substrate at 0, 5, 10, 30, 60, 120, and 180 min with a final overnight sample taken after 19 h. (B) Densitometric analysis of gels. XY scatter plots with diubiquitin percentage plotted against time in minutes for each of the three hUSP11 constructs (as labeled) with each of the eight diubiquitin linkage types (colors indicated in key). Diubiquitin percentage was calculated from ImageJ analyses of SDS-PAGE gels by quantifying the amount of diubiquitin and monoubiquitin in each lane. The mean was calculated from the duplicate assays, and nonlinear regression analyses were performed on time points 0–180 min. Errors are given as standard error mean. ON: overnight sample (not included in nonlinear regression analyses).

The activity of full-length USP11 was assayed using the fluorogenic substrate ubiquitin-AMC (Figure 4C). We observed a K_m of 0.55 μM which is consistent with K_m values reported ranging from 0.12–0.77 μM.[1,16] Comparison of FL-USP11 to the construct lacking the catalytic domain UBL2 containing insert, FLΔUBL2, showed that these constructs display similar kinetic parameters as summarized in Figure 4C. Furthermore, the kinetic parameters for FLΔUBL2 and a construct additionally missing the N-terminal DU domains, CatΔUBL2, were comparable (Figure 4C). The V_{max} and accordingly the k_{cat} values are slightly higher in the FLΔUBL2 protein indicating that removal of the UBL2 insert may lead to a marginal increase in catalytic efficiency. However, a significant inhibitory or activating role for the UBL domains was not observed as reported for other USPs.[47] Deletion of the DU module and UBL2, or the UBL2 containing insert alone, did neither significantly increase nor decrease the K_m compared to the full-length enzyme. Slow conformational changes involving the active site loops are the most likely cause for the sigmoidal kinetic behavior observed with all catalytic domain constructs (Figure 4C), but further investigation is needed to confirm this. This kinetic behavior has also been observed for other USPs.[1] Moreover, we investigated whether the DUSP-UBL domains are able to interact with ubiquitin and did not detect any interaction using ITC or gel filtration (Figure S4, Supporting Information). These data suggest that the catalytic activity of the USP11 protease domain is not modulated through ancillary domains using ubiquitin-AMC as model substrate.

USP11 Displays Specificity for Different Ubiquitin Chain Linkages and This Is Mediated by the Protease Domain. We subsequently investigated the effect of the removal of ancillary USP11 domains on the specificity for diubiquitin substrates of all eight known linkages occurring in the cell. On the basis of diubiquitin chain cleavage time-courses, FL-USP11 displayed little detectable activity for linear chains and highest activity toward Lys^{63}- and Lys^{6}-linked chains. Interestingly, FLΔUBL2 and CatΔUBL2 showed these same preferences (Figure 5). On the basis of these six independent experiments, the eight different diubiquitin linkages can broadly be split into three main groups by preference of all three proteins tested: Lys^{6}- and Lys^{63}-linked chains showed the highest levels of cleavage, Lys^{11}- and Lys^{33}-linked chains showed moderate cleavage, and Lys^{27}-, Lys^{29}-, Lys^{48}-linked and linear chains demonstrated the lowest levels of cleavage. We conducted gel image analysis to further evaluate the data (Figures 5B and S5; Supporting Information). On the basis of

dx.doi.org/10.1021/bi500116x | *Biochemistry* 2014, 53, 2966–2978

the results for all three USP11 catalytic domain constructs investigated, more than 65% of Lys^{63}- and Lys^{6}-linked diubiquitin was cleaved within 3 h and more than 85% after 19 h. FL-USP11 with Lys^{63}-linked and FLΔUBL2 with Lys^{6}-linked chains as substrates showed complete cleavage after 19 h. Lys^{33}- and Lys^{11}-linked chains were cleaved to more than 35% after 3 h and more than 45% after 19 h. Linear, Lys^{48}-, Lys^{29}-, and Lys^{27}-linked diubiquitin chains were cleaved to less than 30% after 3 h and less than 50% even after 19 h.

Two subtle differences were observed between the different constructs tested. Notably, Lys^{27}-linked diubiquitin chains were cleaved to about 50% by FL-USP11 after 19 h. In the same time, FLΔUBL2 and CatΔUBL2 only cleaved about 32% of this substrate. Additionally, for linear diubiquitin virtually no cleavage was observed with FLΔUBL2, whereas FL-USP11 and CatΔUBL2 showed some residual activity (about 10% of the linear diubiquitin was cleaved after 19 h). Taken together, USP11 displays chain specificity, and comparison of FL-USP11 and the deletion mutants indicates that this preference for certain chains is mediated by the protease domain core *in vitro*.

DISCUSSION

It is vital for ubiquitin specific proteases to be able to tightly regulate their catalytic activity as they occupy key positions in important signaling pathways.[48] A range of variable domains are involved in these functions in a number of USPs. For example, UBL domains have been shown to regulate a USP through activation[5,46] and possibly can also inhibit the catalytic activity of USPs, although the latter remains to be confirmed.[18,19,47] The function of USP11 as an important modulator of DNA damage repair is beginning to emerge.[9,10] Here, we undertook an analysis of the USP11 domain structure, investigated the impact of domain deletion mutants on the catalytic function (Figures 4 and 5), and solved the crystal structures of the human and rat USP11 N-terminal DUSP and UBL domains (Figure 1). The monomeric state in solution, molecular envelope, and the presence of the conserved DUSP-UBL interface suggest the formation of the DU finger β-hairpin in hUSP11DU in an analogous way to that observed in the structure of rat USP11DU. Consistent with a DU finger region in hUSP11, asparagine is a favored residue in the i+2 position of type II β-turns.[49] The absence of the protease domain may favor domain swapped dimers under certain conditions and is unlikely to occur in the full length protein that behaves as a monomer. We therefore anticipate that the physiological form of USP11 is a monomer. However, we cannot rule out that conformational changes involving DU finger opening through detachment of the VEVY motif may occur under some conditions as this is observed in our hUSP11 as well as one USP15 DU structure.[24] Through comparison to the homologues USP4 and USP15 (Figures 2 and 3), we have highlighted several novel features in USP11 including: (i) the absence of a pronounced hydrophobic DUSP pocket previously predicted to constitute a protein binding site due to sequence variations in the N-terminal helix and surrounding residues. Differences in this region were even observed between the structures of the closely related species human and rat due to the presence of an additional three residues in the N-terminal helix of human USP11; (ii) significant surface loop variations, especially in the DUSP domain including regions L1 and L2. Although most insertions/deletions occur in the DUSP domain, the adjacent UBL domain is overall even less conserved; (iii) a shortened DU finger region (L4) that lacks a phenylalanine at the tip that may be involved protein−protein interactions in USP4 and USP15. In USP11, residues at the tip of the DU finger are also not conserved across species. These variations are consistent with functional differences, since many of the binding partners for USP4 have also been identified for USP15, whereas binding partners of USP11 are more unique.[45]

Two common structural signature motifs of the DU module found in USP11, USP4, and USP15 can be defined. First, 14 conserved residues including a VEVY motif locate to the interface formed between the linker region and the DUSP domain, highlighting the importance of this interface as a key feature of the DU domain module. USP DU domains are predominantly monomeric in solution and adopt a tandem arrangement of the DUSP and UBL domains including a DU finger β-hairpin. The inherent moderate flexibility between the two domains may indicate that they can have discrete functions as well as acting as one functional unit. Second, the C-terminal part of the UBL domains is characterized by a distinctive loop region not present in other UBL domains including the conserved DGTWP sequence in all members of the DU family.

In total, 7 human USPs harbor DUSP domains[36] and 16 USPs harbor UBL domains, whereby UBL domains nested within the catalytic core are present in eight USPs.[17] UBL domains found in USPs are relatively poorly conserved and a common function is not known. The DUSP domains, although exclusively found in ubiquitin specific proteases, also display a great diversity. and the only common stretch of sequence identified previously, the PGPI motif,[36] does not seem to be important other than for the fold of the DUSP domain.

We show that the USP11 UBL domain displays distinct surface characteristics compared to ubiquitin, but ubiquitin is still a relatively close structural neighbor, despite poor sequence conservation. Since USPs often contain additional ubiquitin binding domains,[3] we also investigated ubiquitin binding to the N-terminal domains. The experiments revealed that the USP11 DU domains do not bind ubiquitin with detectable affinities (Figure S4, Supporting Information) or affect the catalytic efficiency of the enzyme using ubiquitin-AMC as substrate (Figure 4). In addition to N- or C-terminal additional domains, the catalytic core domain of USP family members often contains insertions that encode variable domains.[2] A common insertion point lies close to the distal ubiquitin binding site and was proposed to include an autoinhibitory UBL domain in hUSP4.[18,19] We did not observe an autoregulatory role for the equivalent region in hUSP11 as a construct missing this insert displayed broadly similar kinetic parameters for cleavage of the model substrate Ub-AMC. This shows that in USP11 these domains are not directly involved in regulating the enzymatic activity of the enzyme and highlights the diversity of regulatory mechanisms in USPs. It is still possible that these additional domains of hUSP11 may have a regulatory role through the interaction with other proteins. Such a regulatory function through accessory proteins has been described for some USPs such as USP7, USP1, USP12, and USP46.[1,50,51] The USP11 DU domains and internal UBL2 may also be involved in trafficking or recruiting specific substrates to the catalytic domain.

We show that USP11 preferably cleaves Lys^{63}-, Lys^{6}-, Lys^{33}-, and Lys^{11}-linked ubiquitin chains over Lys^{27}-, Lys^{29}-, Lys^{48}-linked and linear chains. Interestingly, all deletion constructs employed displayed a marked preference for Lys^{63}- and Lys^{6}-linked chains *in vitro*. This is consistent with the DU domains not forming significant interactions with ubiquitin during the

dx.doi.org/10.1021/bi500116x | *Biochemistry* 2014, 53, 2966−2978

catalytic cycle and locates this chain preference to the core protease domain. The ubiquitin chains preferentially cleaved by USP11 adopt quite different conformations. Lys^{63}-linked chains tend to adopt extended conformations,[52,53] whereas Lys^{6}-linked chains are more compact.[54,55] Both, Lys^{63}-linked and linear chains generally adopt relatively open conformations. A high degree of flexibility and the linkage surrounding residues, e.g., the relatively bulky methionine in the linear chain, are likely to account for the differences observed. Interestingly, Lys^{63}- and Lys^{6}-linked ubiquitin chains have been associated with pathways that USP11 has been implicated in,[7,9] namely, DNA damage repair and inflammation,[56] but the functional significance of this *in vivo* remains to be determined. USP11's preferential cleavage of ubiquitin chains is not comparable to the specificity of other deubiquitinating enzymes such as some OTU proteases[57] in that we observed cleavage to some extent with all chains except linear diubiquitin that displayed little cleavage even upon incubation overnight. However, all USP11 constructs consistently showed less activity toward Lys^{27}-, Lys^{29}-, and Lys^{48}-linked and linear chains and as such a clear preference for some chains over others. Taken together, these data advance our understanding of USP11 regulation and function in DNA damage repair pathways and viral infection.

■ ASSOCIATED CONTENT

Supporting Information

Figures S1 (electron densities of the USP11DU linker and DU finger region), S2 (differences in the DUSP domain of USP11, USP4, and USP15), S3 (solution studies of USP11DU and FL-USP11), S4 (hUSP11DU does not detectably associate with ubiquitin in solution), and S5 (densitometric analysis of gels probing ubiquitin chain selectivity with the overnight time point included). This material is available free of charge via the Internet at http://pubs.acs.org.

■ AUTHOR INFORMATION

Corresponding Author

*E-mail: ingrid.dreveny@nottingham.ac.uk. Tel: +44 1158468015. Fax: +44 1158468002.

Author Contributions

#S.H. and H.E.G. contributed equally to the work.

Funding

This work was supported by the Biotechnology and Biological Sciences Research Council through Grant BB/H012656/1 and a studentship to H.E.G., the Royal Society, and the University of Nottingham. Additional support was from the doctoral school "DK Molecular Enzymology" funded by the Austrian Science Fund (FWF) W901-B12.

Notes

The authors declare no competing financial interest.

■ ACKNOWLEDGMENTS

This work was carried out with the support of the ESRF and DESY, and the authors thank beamline staff of beamlines ID23-2, ID29 and X33 for support during data collection. We thank Arie Geerlof (EMBL) for kindly providing the pRSF-13 vector. We thank Hui Lee Tan and Sonal Bakrania for contributions to early experiments and Simon Caulton for helpful suggestions and critically reading the manuscript.

■ ABBREVIATIONS

AMC, 7-amino-4-methylcoumarin; DSC, differential scanning calorimetry; DU, DUSP-UBL; DUSP, domain present in ubiquitin-specific proteases; UBL, ubiquitin-like; USP, ubiquitin specific protease

■ REFERENCES

(1) Faesen, A. C., Luna-Vargas, M. P., Geurink, P. P., Clerici, M., Merkx, R., van Dijk, W. J., Hameed, D. S., El Oualid, F., Ovaa, H., and Sixma, T. K. (2011) The differential modulation of USP activity by internal regulatory domains, interactors and eight ubiquitin chain types. *Chem. Biol. 18*, 1550−1561.

(2) Ye, Y., Scheel, H., Hofmann, K., and Komander, D. (2009) Dissection of USP catalytic domains reveals five common insertion points. *Mol. Biosyst. 5*, 1797−1808.

(3) Reyes-Turcu, F. E., Ventii, K. H., and Wilkinson, K. D. (2009) Regulation and cellular roles of ubiquitin-specific deubiquitinating enzymes. *Annu. Rev. Biochem. 78*, 363−397.

(4) Ventii, K. H., and Wilkinson, K. D. (2008) Protein partners of deubiquitinating enzymes. *Biochem. J. 414*, 161−175.

(5) Fernandez-Montalvan, A., Bouwmeester, T., Joberty, G., Mader, R., Mahnke, M., Pierrat, B., Schlaeppi, J. M., Worpenberg, S., and Gerhartz, B. (2007) Biochemical characterization of USP7 reveals post-translational modification sites and structural requirements for substrate processing and subcellular localization. *FEBS J. 274*, 4256−4270.

(6) Sheng, Y., Saridakis, V., Sarkari, F., Duan, S., Wu, T., Arrowsmith, C. H., and Frappier, L. (2006) Molecular recognition of p53 and MDM2 by USP7/HAUSP. *Nat. Struct. Mol. Biol. 13*, 285−291.

(7) Yamaguchi, T., Kimura, J., Miki, Y., and Yoshida, K. (2007) The deubiquitinating enzyme USP11 controls an IkappaB kinase alpha (IKKalpha)-p53 signaling pathway in response to tumor necrosis factor alpha (TNFalpha). *J. Biol. Chem. 282*, 33943−33948.

(8) Ideguchi, H., Ueda, A., Tanaka, M., Yang, J., Tsuji, T., Ohno, S., Hagiwara, E., Aoki, A., and Ishigatsubo, Y. (2002) Structural and functional characterization of the USP11 deubiquitinating enzyme, which interacts with the RanGTP-associated protein RanBPM. *Biochem. J. 367*, 87−95.

(9) Schoenfeld, A. R., Apgar, S., Dolios, G., Wang, R., and Aaronson, S. A. (2004) BRCA2 is ubiquitinated in vivo and interacts with USP11, a deubiquitinating enzyme that exhibits prosurvival function in the cellular response to DNA damage. *Mol. Cell. Biol. 24*, 7444−7455.

(10) Wiltshire, T. D., Lovejoy, C. A., Wang, T., Xia, F., O'Connor, M. J., and Cortez, D. (2010) Sensitivity to poly(ADP-ribose) polymerase (PARP) inhibition identifies ubiquitin-specific peptidase 11 (USP11) as a regulator of DNA double-strand break repair. *J. Biol. Chem. 285*, 14565−14571.

(11) Maertens, G. N., El Messaoudi-Aubert, S., Elderkin, S., Hiom, K., and Peters, G. (2010) Ubiquitin-specific proteases 7 and 11 modulate Polycomb regulation of the INK4a tumour suppressor. *EMBO J. 29*, 2553−2565.

(12) Liao, T. L., Wu, C. Y., Su, W. C., Jeng, K. S., and Lai, M. M. (2010) Ubiquitination and deubiquitination of NP protein regulates influenza A virus RNA replication. *EMBO J. 29*, 3879−3890.

(13) Lin, C. H., Chang, H. S., and Yu, W. C. (2008) USP11 stabilizes HPV-16E7 and further modulates the E7 biological activity. *J. Biol. Chem. 283*, 15681−15688.

(14) Pedersen, N., Mortensen, S., Sorensen, S. B., Pedersen, M. W., Rieneck, K., Bovin, L. F., and Poulsen, H. S. (2003) Transcriptional gene expression profiling of small cell lung cancer cells. *Cancer Res. 63*, 1943−1953.

(15) Bayraktar, S., Gutierrez Barrera, A. M., Liu, D., Pusztai, L., Litton, J., Valero, V., Hunt, K., Hortobagyi, G. N., Wu, Y., Symmans, F., and Arun, B. (2013) USP-11 as a predictive and prognostic factor following neoadjuvant therapy in women with breast cancer. *Cancer J. 19*, 10−17.

(16) Burkhart, R. A., Peng, Y., Norris, Z. A., Tholey, R., Talbott, V. A., Liang, Q., Ai, Y., Miller, K., Lal, S., Cozzitorto, J. A., Witkiewicz, A.

K., Yeo, C. J., Gehrmann, M., Napper, A., Winter, J. M., Sawicki, J. A., Zhuang, Z., and Brody, J. R. (2013) Mitoxantrone targets human ubiquitin-specific peptidase 11 (USP11) and is a potent inhibitor of pancreatic cancer cell survival. *Mol. Cancer Res. 11*, 901−911.
(17) Zhu, X., Menard, R., and Sulea, T. (2007) High incidence of ubiquitin-like domains in human ubiquitin-specific proteases. *Proteins 69*, 1−7.
(18) Luna-Vargas, M. P., Faesen, A. C., van Dijk, W. J., Rape, M., Fish, A., and Sixma, T. K. (2011) Ubiquitin-specific protease 4 is inhibited by its ubiquitin-like domain. *EMBO Rep. 12*, 365−372.
(19) Luna-Vargas, M. P., Faesen, A. C., Van Dijk, W. J., Rape, M., Fish, A., and Sixma, T. K. (2014) Retraction:'Ubiquitin-specific protease 4 is inhibited by its ubiquitin-like domain. *EMBO Rep. 15*, 121.
(20) Song, E. J., Werner, S. L., Neubauer, J., Stegmeier, F., Aspden, J., Rio, D., Harper, J. W., Elledge, S. J., Kirschner, M. W., and Rape, M. (2010) The Prp19 complex and the Usp4Sart3 deubiquitinating enzyme control reversible ubiquitination at the spliceosome. *Genes Dev. 24*, 1434−1447.
(21) Zhao, B., Velasco, K., Sompallae, R., Pfirrmann, T., Masucci, M. G., and Lindsten, K. (2012) The ubiquitin specific protease-4 (USP4) interacts with the S9/Rpn6 subunit of the proteasome. *Biochem. Biophys. Res. Commun. 427*, 490−496.
(22) Hayes, S. D., Liu, H., MacDonald, E., Sanderson, C. M., Coulson, J. M., Clague, M. J., and Urbe, S. (2012) Direct and indirect control of mitogen-activated protein kinase pathway-associated components, BRAP/IMP E3 ubiquitin ligase and CRAF/RAF1 kinase, by the deubiquitylating enzyme USP15. *J. Biol. Chem. 287*, 43007−43018.
(23) Harper, S., Besong, T. M., Emsley, J., Scott, D. J., and Dreveny, I. (2011) Structure of the USP15 N-terminal domains: a beta-hairpin mediates close association between the DUSP and UBL domains. *Biochemistry 50*, 7995−8004.
(24) Elliott, P. R., Liu, H., Pastok, M. W., Grossmann, G. J., Rigden, D. J., Clague, M. J., Urbe, S., and Barsukov, I. L. (2011) Structural variability of the ubiquitin specific protease DUSP-UBL double domains. *FEBS Lett. 585*, 3385−3390.
(25) Hu, M., Li, P., Song, L., Jeffrey, P. D., Chenova, T. A., Wilkinson, K. D., Cohen, R. E., and Shi, Y. (2005) Structure and mechanisms of the proteasome-associated deubiquitinating enzyme USP14. *EMBO J. 24*, 3747−3756.
(26) Gorrec, F. (2009) The MORPHEUS protein crystallization screen. *J. Appl. Crystallogr. 42*, 1035−1042.
(27) Collaborative Computational Project, N. (1994) The CCP4 suite: programs for protein crystallography, *Acta Crystallogr. D Biol. Crystallogr. 50*, 760−763.
(28) McCoy, A. J., Grosse-Kunstleve, R. W., Adams, P. D., Winn, M. D., Storoni, L. C., and Read, R. J. (2007) Phaser crystallographic software. *J. Appl. Crystallogr. 40*, 658−674.
(29) Adams, P. D., Afonine, P. V., Bunkoczi, G., Chen, V. B., Davis, I. W., Echols, N., Headd, J. J., Hung, L. W., Kapral, G. J., Grosse-Kunstleve, R. W., McCoy, A. J., Moriarty, N. W., Oeffner, R., Read, R. J., Richardson, D. C., Richardson, J. S., Terwilliger, T. C., and Zwart, P. H. (2010) PHENIX: a comprehensive Python-based system for macromolecular structure solution. *Acta Crystallogr. D Biol. Crystallogr. 66*, 213−221.
(30) Painter, J., and Merritt, E. A. (2006) Optimal description of a protein structure in terms of multiple groups undergoing TLS motion. *Acta Crystallogr. D Biol. Crystallogr. 62*, 439−450.
(31) Kabsch, W. (2010) Xds. *Acta Crystallogr. D Biol. Crystallogr. 66*, 125−132.
(32) Konarev, P. V., Petoukhov, M. V., Volkov, V. V., and Svergun, D. I. (2006) ATSAS 2.1, a program package for small-angle scattering data analysis. *J. Appl. Crystallogr. 39*, 277−286.
(33) Svergun, D. I. (1992) Determination of the regularization parameter in indirect-transform methods using perceptual criteria. *J. Appl. Crystallogr. 25*, 495−503.
(34) Pettersen, E. F., Goddard, T. D., Huang, C. C., Couch, G. S., Greenblatt, D. M., Meng, E. C., and Ferrin, T. E. (2004) UCSF Chimera–a visualization system for exploratory research and analysis. *J. Comput. Chem. 25*, 1605−1612.
(35) Yang, Z. R., Thomson, R., McNeil, P., and Esnouf, R. M. (2005) RONN: the bio-basis function neural network technique applied to the detection of natively disordered regions in proteins. *Bioinformatics 21*, 3369−3376.
(36) de Jong, R. N., Ab, E., Diercks, T., Truffault, V., Daniels, M., Kaptein, R., and Folkers, G. E. (2006) Solution structure of the human ubiquitin-specific protease 15 DUSP domain. *J. Biol. Chem. 281*, 5026−5031.
(37) Krissinel, E., and Henrick, K. (2007) Inference of macromolecular assemblies from crystalline state. *J. Mol. Biol. 372*, 774−797.
(38) Holm, L., and Sander, C. (1995) Dali: a network tool for protein structure comparison. *Trends Biochem. Sci. 20*, 478−480.
(39) Vijay-Kumar, S., Bugg, C. E., and Cook, W. J. (1987) Structure of ubiquitin refined at 1.8 Å resolution. *J. Mol. Biol. 194*, 531−544.
(40) Dreveny, I., Kondo, H., Uchiyama, K., Shaw, A., Zhang, X., and Freemont, P. S. (2004) Structural basis of the interaction between the AAA ATPase p97/VCP and its adaptor protein p47. *EMBO J. 23*, 1030−1039.
(41) Aggarwal, K., and Massague, J. (2012) Ubiquitin removal in the TGF-beta pathway. *Nat. Cell Biol. 14*, 656−657.
(42) Al-Salihi, M. A., Herhaus, L., Macartney, T., and Sapkota, G. P. (2012) USP11 augments TGFbeta signalling by deubiquitylating ALK5. *Open Biol. 2*, 120063.
(43) Eichhorn, P. J., Rodon, L., Gonzalez-Junca, A., Dirac, A., Gili, M., Martinez-Saez, E., Aura, C., Barba, I., Peg, V., Prat, A., Cuartas, I., Jimenez, J., Garcia-Dorado, D., Sahuquillo, J., Bernards, R., Baselga, J., and Seoane, J. (2012) USP15 stabilizes TGF-beta receptor I and promotes oncogenesis through the activation of TGF-beta signaling in glioblastoma. *Nat. Med. 18*, 429−435.
(44) Zhang, L., Zhou, F., Drabsch, Y., Gao, R., Snaar-Jagalska, B. E., Mickanin, C., Huang, H., Sheppard, K. A., Porter, J. A., Lu, C. X., and ten Dijke, P. (2012) USP4 is regulated by AKT phosphorylation and directly deubiquitylates TGF-beta type I receptor. *Nat. Cell Biol. 14*, 717−726.
(45) Sowa, M. E., Bennett, E. J., Gygi, S. P., and Harper, J. W. (2009) Defining the human deubiquitinating enzyme interaction landscape. *Cell 138*, 389−403.
(46) Faesen, A. C., Dirac, A. M., Shanmugham, A., Ovaa, H., Perrakis, A., and Sixma, T. K. (2011) Mechanism of USP7/HAUSP activation by its C-terminal ubiquitin-like domain and allosteric regulation by GMP-synthetase. *Mol. Cell 44*, 147−159.
(47) Faesen, A. C., Luna-Vargas, M. P., and Sixma, T. K. (2012) The role of UBL domains in ubiquitin-specific proteases. *Biochem. Soc. Trans. 40*, 539−545.
(48) Kim, J. H., Park, K. C., Chung, S. S., Bang, O., and Chung, C. H. (2003) Deubiquitinating enzymes as cellular regulators. *J. Biochem 134*, 9−18.
(49) Hutchinson, E. G., and Thornton, J. M. (1994) A revised set of potentials for beta-turn formation in proteins. *Protein Sci. 3*, 2207−2216.
(50) van der Knaap, J. A., Kumar, B. R., Moshkin, Y. M., Langenberg, K., Krijgsveld, J., Heck, A. J., Karch, F., and Verrijzer, C. P. (2005) GMP synthetase stimulates histone H2B deubiquitylation by the epigenetic silencer USP7. *Mol. Cell 17*, 695−707.
(51) Cohn, M. A., Kee, Y., Haas, W., Gygi, S. P., and D'Andrea, A. D. (2009) UAF1 is a subunit of multiple deubiquitinating enzyme complexes. *J. Biol. Chem. 284*, 5343−5351.
(52) Varadan, R., Assfalg, M., Haririnia, A., Raasi, S., Pickart, C., and Fushman, D. (2004) Solution conformation of Lys63-linked di-ubiquitin chain provides clues to functional diversity of polyubiquitin signaling. *J. Biol. Chem. 279*, 7055−7063.
(53) Komander, D., Reyes-Turcu, F., Licchesi, J. D., Odenwaelder, P., Wilkinson, K. D., and Barford, D. (2009) Molecular discrimination of structurally equivalent Lys 63-linked and linear polyubiquitin chains. *EMBO Rep 10*, 466−473.

(54) Virdee, S., Ye, Y., Nguyen, D. P., Komander, D., and Chin, J. W. (2010) Engineered diubiquitin synthesis reveals Lys29-isopeptide specificity of an OTU deubiquitinase. *Nat. Chem. Biol. 6*, 750−757.
(55) Fushman, D., and Walker, O. (2010) Exploring the linkage dependence of polyubiquitin conformations using molecular modeling. *J. Mol. Biol. 395*, 803−814.
(56) Chen, Z. J., and Sun, L. J. (2009) Nonproteolytic functions of ubiquitin in cell signaling. *Mol. Cell 33*, 275−286.
(57) Mevissen, T. E., Hospenthal, M. K., Geurink, P. P., Elliott, P. R., Akutsu, M., Arnaudo, N., Ekkebus, R., Kulathu, Y., Wauer, T., El Oualid, F., Freund, S. M., Ovaa, H., and Komander, D. (2013) OTU deubiquitinases reveal mechanisms of linkage specificity and enable ubiquitin chain restriction analysis. *Cell 154*, 169−184.